THE INFLUENCE OF THE BLADE FEATHER CONSTRUCTIONAL INHOMOGENEITY ON THE TURBINE COOLING BLADES STRESS-STRAIN STATE

Досліджено вплив конструктивної неоднорідності пера лопаток турбомашин на напружено-деформований стан. Встановлено вплив геометричних параметрів порожнини пера на величину максимальних динамічних напружень та зони локалізації в охолоджуваних лопатках газових турбін. Визначено механізм формування поля динамічних напружень в пері лопатки, спричиненого комплексною дією вібраційного та теплового навантажень

Ключові слова: лопатки турбомашин, геометричні параметри пера, тривимірні скінчені елементи, динамічні напруження

Исследовано влияние конструктивной неоднородности пера лопаток турбомашин на напряженно-деформированное состояние. Установлено влияние геометрических параметров полости пера на величину максимальных динамических напряжений и зоны локализации в охлаждаемых лопатках газовых турбин. Определен механизм формирования поля динамических напряжений в пере лопатки, вызванного комплексным воздействием вибрационной и тепловой нагрузок

Ключевые слова: лопатки турбомашин, геометрические параметры пера, трехмерные конечные элементы, динамические напряжения

S. Morhun
PhD
Department of engineering mechanics and technology of machine building
Admiral Makarov National University of Shipbuilding
Heroiv Ukrainy ave. 9,
Mykolaiv, Ukraine, 54025
E-mail: serhii.morhun@nuos.edu.ua

1. Introduction

Nowadays one of the main trends in the power machine building area is a steady increase of turbine engines power. On the other hand, this trend should also be complemented by an increase of whole turbines and their main assembly units reliability and durability. That is why, for the purpose of marine gas turbine engines trouble-free operations, we need to study vibration processes, which influence sharply reduces the durability of the whole turbine. Special attention should be paid to the turbine rotor blades, heavily loaded by the non-stationary gas flow. Furthermore, we should also take into consideration such aspect as an extremely high temperature of gas flow. All these negative factors cause the complex influence of vibration and thermal loads on the blades surfaces.

Due to the high cost of modern turbines and especially the processes of their debugging, it is extremely important to use the proper numerical methods for the blades vibration characteristics and stress-strain state calculation. That is why the complex investigation of gas turbine blades vibration and stress-strain state is an essential scientific and practical problem. So, despite intense researches in this field [1, 2], there are several uncovered important aspects.

According to the sharp and steady increase of modern marine vehicles gas turbine engines power, the problem of their blades stress-strain investigation is rather actual.

2. Literature review and problem statement

In modern literature, the issues of gas turbine blades correct design are linked with the finite element method (FEM) usage. In the paper [3], not only non-cooled, but also cooled turbine blades models on the base of FEM are given. But the main disadvantage of these models is an incorrect description of blades feather and its cavity by the plane finite elements of triangular type. These circumstances sharply decrease the reliability of the obtained results. To prevent all the aforementioned disadvantages, in the papers [4–6] the three-dimensional finite element models are used. For example, in [4] special four-node finite elements of shell type were applied for the blades feather modeling. For the blades bandage modeling, the eight-node finite elements of prismatic type were also used. In the paper [5], the authors simulate the blade's feather using the eight-node finite elements of prismatic type and in the paper [6] – four-node finite elements of sector type.

In [7, 8], this problem of turbine blades stress-strain state calculation is also solved by means of FEM, but in [7] the damping is not taken into consideration. In the paper [8], the mathematical model of the steam turbine blade is built on the base of tetrahedral finite elements. But such type of elements can't correctly describe constructional non-homogeneity of blade's feather and especially its cooling cavity.

Some of these works [5, 8] deal with the research of single crystal turbine blades stress-strain state. For example, in the

paper [5] the processes of the thermal stresses field formation have been studied, but the blades feather temperature field is shown holonomic. The problem of blade feather uneven heat is not taken into consideration. In [8], the field of equivalent dynamic stresses in the compressor blade is given. But for the rotor blades of marine gas turbine engines, made of the heat-resistant alloys on the base of nickel and cobalt, the technology of single crystal blades manufacturing is not put into production. That's why the numerical results given in the papers [5, 8] can't be taken as a base for the marine gas turbine blades stress-strain state research.

There are also several experimental methodologies that could be applied for the research of dynamic stresses on the blade's surface [9]. But all these methodologies are very expensive and less reliable due to the systematic error of measuring equipment that can't be excluded.

3. The aim and objectives of the study

The main aim of the work is to research an influence of the turbine blades feather constructional non-homogeneity on the stress-strain state, caused by the complex effect of vibration and thermal loads.

To achieve the aim, the following tasks have been considered:
– to develop a more correct mathematical model of the constructional non-homogeneous turbine blades stress-strain state on the base of three-dimensional curvilinear finite elements;
– to study the influence of the blade's feather constructional parameters on their localization zones location and the value of maximum dynamic stresses on the blades surface;
– to compare the calculated results with the experimental data to take a decision about an adequacy of the designed mathematical model.

4. Materials and methodology of the study of the cooling turbine blades stress-strain state

The mathematical model of the gas turbine cooling blade of an asymmetric transverse section, located in the right rectangular Cartesian coordinate system is given (Fig. 1).
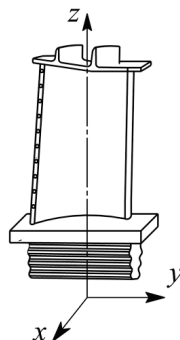

Fig. 1. Three-dimensional model of the gas turbine cooling blade

The investigated gas turbine cooling blade is located in the right rectangular Cartesian coordinate system xyz. The z axis is normal to the turbine rotor axis of rotation; x matches the turbine rotor axis of rotation. The whole coor-

dinate system is rotating with constant angular velocity Ω together with the rotor.

The oscillations of the three-dimensional finite element model of a solid body, shown in Fig. 1, can be described by the Lagrange variation principle [10–13]:

$$\frac{\partial L}{\partial q_i} - \frac{d}{dt}\left(\frac{\partial L}{\partial \dot{q}_i}\right) = 0, \quad i = (1,...,n), \tag{1}$$

where $L = \Pi - T$ – Lagrange function; Π – potential energy of the finite element resistance to deformation; T – kinetic energy of the finite element oscillation; q_i – generalized coordinates of the element's node i; n – the quantity of the nodes for each element.

On the base of the dependencies, given in the papers [11, 13], the potential energy of the finite element resistance to deformation can be calculated in the following way:

$$\Pi = \frac{1}{2}\iiint_V \varepsilon^T D_\sigma \varepsilon dV = \frac{1}{2}\iiint_V B^T DB dV = \frac{1}{2}\left(\delta^T K \delta\right), \tag{2}$$

where K – stiffness matrix of the finite element; δ – vector of the finite element nodes generalized displacement.

Kinetic energy of the finite element oscillation can be obtained as follows:

$$T = \frac{1}{2}\iiint_V \rho \delta^T B^T N^T BN \delta dV = \frac{1}{2}\left(\delta^T M \delta\right), \tag{3}$$

where M – mass matrix of the finite element.

4. 1. Description of the finite elements, modeling the gas turbine blade feather

We need to say that according to the gas turbine blade geometry, its feather should be considered as a space solid body, which surfaces have a complicated curvilinear form. That's why its correct modeling can be achieved only by the usage of specially designed curvilinear three-dimensional finite elements, which shape should be equidistant to the feather surface. Other constructional units of the blade, like its bandage or shank, can be satisfactorily described by a number of standard eight-node finite elements of hexagonal type that are present in the FEM libraries of ANSYS, MATHLAB and other programming environments [14].

The designed curvilinear finite element has its own local coordinate system ξ, ζ, η (Fig. 2). Transfer from the global Cartesian coordinate system xyz of the whole blade to the finite element's local coordinate system ζ, η, ξ can be described by the dependencies:

$$\begin{Bmatrix} x \\ y \\ z \end{Bmatrix} = \sum N_i(\xi,\eta)\frac{1+\zeta}{2}\begin{Bmatrix} x_i \\ y_i \\ z_i \end{Bmatrix} + \sum N_i(\xi,\eta)\frac{1-\zeta}{2}\begin{Bmatrix} x_i \\ y_i \\ z_i \end{Bmatrix},$$
$$i = (1,2,...,8), \tag{4}$$

where (x, y, z) – global Cartesian coordinates of the element; (x_i, y_i, z_i) – Cartesian coordinates of the node i; (ζ, ξ, η) – curvilinear local coordinates of the element; $N_i(\eta, \xi)$ – finite element's shape functions.

In the dependences (4) and further, we need to use the procedure of shape functions summarizing according to the repeated indexes. Shape functions of the developed curvilinear finite element are represented by the dependencies (5):

$$N_1 = \frac{1}{4}(1-\eta)(1-\xi)(-\xi-\eta-1); \quad N_2 = \frac{1}{2}(1-\eta)(1-\xi^2);$$

$$N_3 = \frac{1}{4}(1-\eta)(1+\xi)(\xi-\eta-1); \quad N_4 = \frac{1}{2}(1-\eta^2)(1+\xi);$$

$$N_5 = \frac{1}{4}(1+\eta)(1+\xi)(\xi+\eta-1); \quad N_6 = \frac{1}{2}(1+\eta)(1-\xi^2);$$

$$N_7 = \frac{1}{4}(1+\eta)(1+\xi)(-\xi+\eta-1); \quad N_8 = \frac{1}{2}(1-\eta^2)(1-\xi). \quad (5)$$
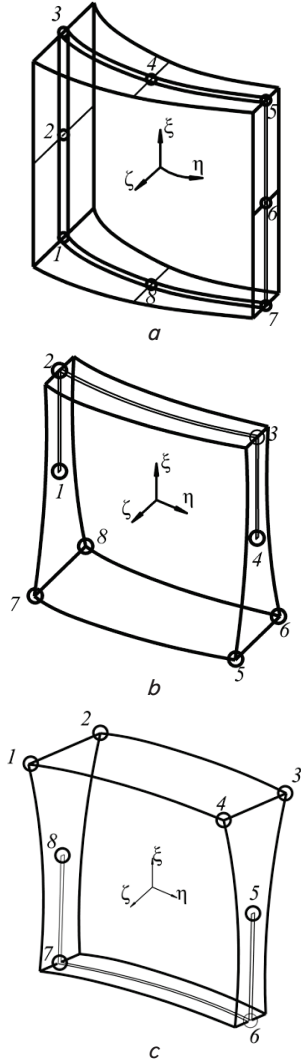

Fig. 2. Modifications of the three-dimensional finite element:
a — curvilinear finite element, modeling the blade's feather;
b — element, modeling the transition zone from feather
to shank; *c* — element, modeling the transition zone from
feather to bandage

Generalized displacements of the finite element's nodes in the directions *x, y, z* can be calculated on the base of dependencies (4) and (5):

$$u = \sum N_i(\eta,\xi)u_i + \sum N_i(\eta,\xi)\zeta\frac{h_i}{2}\left(\mathbf{v}_i^1\alpha_i^1 - \mathbf{v}_i^2\alpha_i^2\right),$$

$$(i = 1, 2,..., 8), \quad (6)$$

where u_i – displacement vector of the finite element i node; h_i – finite element thickness in the i node location; $\mathbf{v}^1$ and $\mathbf{v}^2$ – orthonormal vectors in the i node to the

element's middle surface; α^1 and α^2 – rotational angles of the normal to the element's middle surface in the i node.

The generalized displacement vector of the blade's feather finite element model is formed according to the dependencies (7):

$$\delta = \begin{Bmatrix} u_1 \\ u_2 \\ \vdots \\ u_m \end{Bmatrix}, \quad (7)$$

where m – quantity of the finite elements, forming the blade's feather model.

4. 2. The influence of the vibration load on the turbine blade feather field of displacement

Appearance of the dynamic stresses field on the turbine blade feather surface is caused by a complex influence of vibration and thermal loads [10, 12, 13]. First, let us study the influence of the vibration load on the blade feather field of displacement.

The cooling turbine blade forced vibration, caused by the k harmonic of the gas-dynamic force equation is given below:

$$[M]\left\{\frac{d^2\delta}{dt^2}\right\} + [C]\left\{\frac{d\delta}{dt}\right\} + [K]\{\delta\} = \{F\}, \quad (8)$$

where C – matrix of damping; δ – generalized displacement vector of the blade's feather finite element model; F – vector of the vibration load.

The methodology of calculation of the vibration load, caused by the influence of gas flow on the turbine blade surface has been given in [15].

The solution of the equation (8) can be found in the following way:

$$\delta_J = a_J^1 \cos k\Omega t + a_J^2 \sin k\Omega t, \quad (J=1,2,...,n, \, k=1,....,g), \quad (9)$$

where g – number of the vibration load harmonics; n – quantity of the finite element model nodes.

To calculate the blade forced vibration amplitudes a_J^1 and a_J^2, we need to solve the system of equations (10), formed by the unity of the dependences (8) and (9):

$$M_{IJ}\left(a_J^{(1)}\cos k\Omega t + a_J^{(2)}\sin k\Omega t\right)'' +$$

$$+ C_{IJ}\left(a_J^{(1)}\cos k\Omega t + a_J^{(2)}\sin k\Omega t\right)' +$$

$$+ K_{IJ}\left(a_J^{(1)}\cos k\Omega t + a_J^{(2)}\sin k\Omega t\right) =$$

$$= F_I^{(1)}\cos k\Omega t + F_I^{(2)}\sin k\Omega t, \, (I, J = 1,2,...,n). \quad (10)$$

Here and in the next equations, we will use the index (1) to mark the terms of equation with $\cos k\Omega t$. Index (2) should be used to mark the terms of equation with $\sin k\Omega t$.

By transforming the system (10), we receive two systems of equations (11) – with $\cos k\Omega t$ and (12) – with $\sin k\Omega t$:

$$\Lambda_{11}a_1^{(1)} + \Lambda_{10}a_0^{(1)} + \Lambda_{12}a_2^{(1)} + \Psi_{11}a_1^{(2)} + \Psi_{10}a_0^{(2)} + \Psi_{12}a_2^{(2)} = F_1^{(1)};$$

$$\Lambda_{01}a_1^{(1)} + \Lambda_{00}a_0^{(1)} + \Lambda_{02}a_2^{(1)} + \Psi_{01}a_1^{(2)} + \Psi_{00}a_0^{(2)} + \Psi_{02}a_2^{(2)} = F_0^{(1)};$$

$$\Lambda_{21}a_1^{(1)} + \Lambda_{20}a_0^{(1)} + \Lambda_{22}a_2^{(1)} + \Psi_{21}a_1^{(2)} + \Psi_{20}a_0^{(2)} + \Psi_{22}a_2^{(2)} = F_2^{(1)}, \quad (11)$$

$$-\Psi_{11}a_1^{(1)} - \Psi_{10}a_0^{(1)} - \Psi_{12}a_1^{(2)} + \Lambda_{11}a_1^{(2)} + \Lambda_{10}a_0^{(2)} + \Lambda_{12}a_2^{(2)} = F_1^{(2)};$$

$$-\Psi_{01}a_1^{(1)} - \Psi_{00}a_0^{(1)} - \Psi_{02}a_1^{(2)} + \Lambda_{01}a_1^{(2)} + \Lambda_{00}a_0^{(2)} + \Lambda_{02}a_2^{(2)} = F_0^{(2)};$$

$$-\Psi_{21}a_1^{(1)} - \Psi_{20}a_0^{(1)} - \Psi_{22}a_1^{(2)} + \Lambda_{21}a_1^{(2)} + \Lambda_{20}a_0^{(2)} + \Lambda_{22}a_2^{(2)} = F_2^{(2)}, \quad (12)$$

where $\Psi_{IJ} = k\Omega C_{IJ}$, and $\Lambda_{IJ} = K_{IJ} - (k\Omega^2)M_{IJ}$; Λ_{11}, Λ_{01}, Λ_{21}, etc. – units of the dynamic stiffness matrix. Index 1 marks the nodes, located on the blade feather leading edge; index 0 marks the nodes, located on the feather central part and index 2 marks the nodes, located on the feather output edge. For the dynamic matrix of damping Ψ, the same designations can be used; $a_1^{(1)}$, $a_0^{(1)}$, $a_2^{(1)}$ etc – forced vibration amplitudes of the nodes, located on the blade feather leading edge, central part and output edge.

The unity of systems (11) and (12) gives us the resolving system of matrix equations:

$$[S] \begin{Bmatrix} a_1^{(1)} \\ a_0^{(1)} \\ a_2^{(1)} \\ a_1^{(2)} \\ a_0^{(2)} \\ a_2^{(2)} \end{Bmatrix} = \begin{Bmatrix} F_1^{(1)} \\ F_0^{(1)} \\ F_2^{(1)} \\ F_1^{(2)} \\ F_0^{(2)} \\ F_2^{(2)} \end{Bmatrix}. \quad (13)$$

Matrix S is formed from the units of the dynamic stiffness matrix.

4. 3. Formation of the blade feather field of temperatures

The temperature state of the solid body caused by the convective heat transfer without any internal heat sources could be reduced to the next variation equation [16]:

$$\delta J_T = 0.$$

As the turbine blade model is located in the Cartesian coordinate system, then the temperature functional J_T can be found in the following way:

$$J_T = \frac{1}{2}\int_V \lambda\left[\left(\frac{\partial T}{\partial x}\right)^2 + \left(\frac{\partial T}{\partial y}\right)^2 + \left(\frac{\partial T}{\partial z}\right)^2\right]dV +$$

$$+ \frac{1}{2}\int_S h(T - T_0)^2\,dS, \quad (14)$$

where T – temperature of the turbine blade material; T_0 – temperature of the gas flow; λ – thermal conductivity coefficient; h – heat exchange coefficient; V – volume of the blade.

After the FEM approximation, the dependencies (14) should be transformed in this way:

$$J_{Te} = \frac{1}{2}\int_{Ve}(T_e)^T B_e{}^T D B_e T_e\,dV_e + \frac{1}{2}\int_S h_e(T_e - T_{0e})^2\,dS_e,$$

$$(e = 1, 2,..., m), \quad (15)$$

where T_e – matrix of the blade material temperature within the finite element e; T_{0e} – matrix of the gas flow temperature, contacting with the surface of the finite element e; B_e – matrix of gradients for the finite element e; D – elasticity matrix

of the blade material; m – the quantity of the finite elements, forming the blade feather model.

So, the vector of temperatures for any finite element e, modeling the blade feather can be defined:

$$T_e = NT = \begin{bmatrix} N_i & N_j & \dots & N_n \end{bmatrix}^T \begin{Bmatrix} T_i \\ T_j \\ \vdots \\ T_n \end{Bmatrix},$$

$$(i = 1, 2,..., n), \quad (16)$$

where $T_i...T_n$ – temperatures in the nodes of the finite element e.

4. 4. Calculation of the dynamic stresses on the turbine blade feather surface

Let us calculate the components of the dynamic stresses matrix. Firstly, we need to find the potential energy of the blade feather deformation using the dependences (2). So, we will receive the following equation:

$$\Pi = \frac{1}{2}\iiint_V \begin{bmatrix} \sigma_x(\varepsilon_x - \varepsilon_{xT}) + o_y(\varepsilon_y - \varepsilon_{yT}) + \\ + \sigma_z(\varepsilon_z - \varepsilon_{zT}) + \tau_{xy}\gamma_{xy} + \\ + \tau_{xz}\gamma_{xz} + \tau_{zy}\gamma_{zy} \end{bmatrix} dxdydz, \quad (17)$$

where ε_x, ε_y, ε_z, γ_{xy}, γ_{xz}, γ_{zy} – components of the elastic deformation matrix; ε_{xT}, ε_{yT}, ε_{zT} – components of the thermal deformation matrix.

The matrix of the blade feather thermal deformation ε_T can be formed on the base of dependences (15)–(16) and has the following structure:

$$\varepsilon_T = \begin{Bmatrix} \alpha T & \alpha T & \alpha T & 0 & 0 & 0 \end{Bmatrix}^T, \quad (18)$$

where α – coefficient of the blade material extension.

The matrix of elastic deformation ε can be formed similarly to the matrix ε_T and has the following structure:

$$\{\varepsilon\} = \begin{Bmatrix} \varepsilon_x & \varepsilon_y & \varepsilon_z & \gamma_{xy} & \gamma_{xz} & \gamma_{yz} \end{Bmatrix}^t =$$

$$= \begin{Bmatrix} \frac{\partial \delta_x}{\partial x} & \frac{\partial \delta_y}{\partial y} & \frac{\partial \delta_z}{\partial z} & \frac{\partial \delta_x}{\partial y} + \frac{\partial \delta_y}{\partial x} & \frac{\partial \delta_x}{\partial z} + \frac{\partial \delta_z}{\partial x} & \frac{\partial \delta_y}{\partial z} + \frac{\partial \delta_z}{\partial y} \end{Bmatrix}^t, (19)$$

where δ_x, δ_y, δ_z – components of the generalized displacement vector, describing the blade feather finite elements model nodes displacement.

Then on the base of dependencies (18) and (19), the matrix of dynamic stresses is formed:

$$\{\sigma\} = \begin{Bmatrix} \sigma_x \\ \sigma_y \\ \sigma_z \\ \tau_{xy} \\ \tau_{xz} \\ \tau_{yz} \end{Bmatrix} = [D](\{\varepsilon\} - \{\varepsilon_T\}). \quad (20)$$

Usage of this mathematical model gives us an opportunity to calculate the field of dynamic stresses on the turbine blade feather surface for any mode of the blade's oscillation, because application of the dependences (9)–(13) gives an opportunity to take into consideration any k-th harmonic of the vibration load.

5. Results of the turbine blade stress-strain state determining and analysis

In Fig. 3, the localization zones of the dynamic stresses situated on the cooling turbine blade feather external and internal surfaces are shown. The blade is made out of high-temperature alloy X2 CrNiMo 17-14-3. The first bending mode of the blade forced oscillation is taken into consideration ($\Omega = 1382$ Hz).
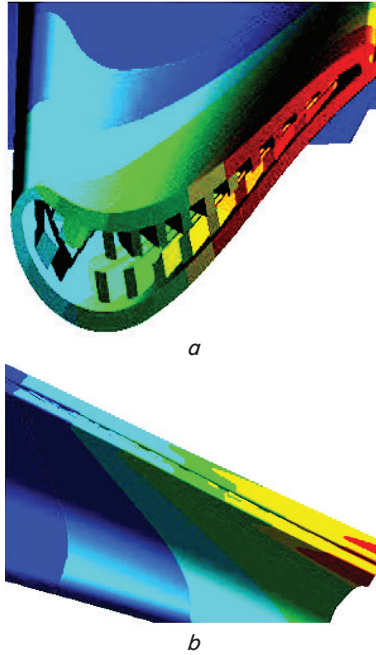

a

b

Fig. 3. Localization zones of dynamic stresses on the cooling blade feather surface for the first bending oscillation mode: *a* — in the blade cavity transverse section; *b* — on the blade output edge

According to the dynamic stresses zones localization (Fig. 3), specific to the first bending mode of the turbine blade vibration, it has been found that for the turbine constructional non-homogenous cooling blade feather, the extremes of the stresses are located near the cooling holes on the blade output edge and on the internal surface of cooling channels. (These zones are highlighted by red color in Fig. 3. Other colors in the range show the reduction of the dynamic stresses value). This can be explained by the fact that the cooling holes are the stress concentrators. The transition zones from cooling channels, located in the cavity, to the feather internal surface also are stress concentrators. It is rather difficult technologically to provide the smoothness of transition between the surfaces of cooling channels walls and the feather. So, according to the maximum dynamic stresses location, next we will study the influence of the blade cavity and output edge constructional parameters (Fig. 4) on these stresses value.

The material of the investigated turbine cooling blade is heat resistant alloy X2 CrNiMo 17-14-3, which has the following parameters: density $\rho = 8100$ kg/m³; Young's modulus $E = 1.79 \cdot 10^6$ MPa; Poison's ratio $\upsilon = 0.3$ [17].

For taking the decision about the developed mathematical model adequacy, we should compare the calculated results with the experimental data. The experimental methodology is given in the paper [17].
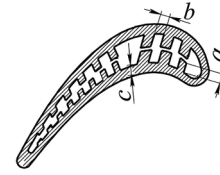

Fig. 4. Cross section of turbine blade feather's cavity with its geometric parameters

Let us study the influence of the blade feather thickness *c* on the value of maximum dynamic stresses on its surface (Fig. 5).
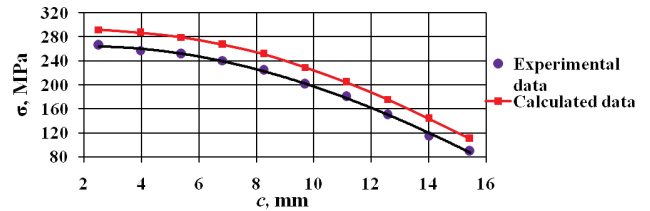

Fig. 5. Influence of the blade feather thickness *c* on the value of maximum dynamic stresses σ on its surface

Graphic data, shown in Fig. 5, gives us an opportunity to make a conclusion that the value of maximum dynamic stresses is reduced due to the increase of the blade feather thickness. Explanation of this fact is that the increase of feather thickness also causes the increase of its cross-sectional area.

Some results of the research are represented in Table 1, 2. They show the influence of the cooling channels geometric parameters on the value of maximum dynamic stresses on the blades feather internal surface.

Table 1

Influence of the cooling channels walls thickness *b* on the value of maximum dynamic stresses

Cooling channels walls thickness *b*, mm	Maximum dynamic stresses value σ, MPa	
	Calculated data	Experimental data
1.5	261.4	256
2.0	255.8	247
2.5	241.5	235
3.0	233.2	227

Table 2

Influence of the cooling channels walls height *a* on the value of maximum dynamic stresses

Cooling channels walls height *a*, mm	Maximum dynamic stresses value σ, MPa	
	Calculated data	Experimental data
5.0	284.2	280
8.0	271.9	267
10.0	263.7	256
12.0	252.9	248
15.0	241.4	236

The data represented in Table 1 shows us that the increase of the cooling channels walls thickness causes a decrease of the dynamic stresses value. The matter is that when

studying such constructional parameters of the blade cavity as a net of cooling channels we need to consider their walls as a number of stiffening ribs for the shells. Then, according to the thin shells theory of Kirghoff- Lyav, we can affirm that the increase of the walls thickness value causes an increase of the whole blade feather stiffness and as a result reduces the dynamic stresses value.

The increase of the cooling channels walls height (Table 2) causes a slight decrease of the dynamic stresses value too. The matter is that if the channels walls are higher, then the walls cross-sectional area grows. This fact causes the increases of the blade feather stiffness and as a result – decrease of the dynamic stresses value.

But, as it was postulated above, the main zones of maximum dynamic stresses localization are not only in the blade feather cavity but also on the blade output edge. The main stress concentrators on the output edge surface are the cooling holes of different geometric form: circular, square and elliptic. We should study the influence of the circular cooling holes on the dynamic stresses value, because such form of the cooling holes is the most widespread in the marine gas turbine engines.

The data, given in Table 3 and 4 shows the influence of the diameter of the cooling holes, located on the turbine blade output edge, on the dynamic stresses value.

Table 3

Influence of the cooling holes quantity q on the value of maximum dynamic stresses on the blade output edge

Quantity of holes q	Maximum dynamic stresses value σ, MPa	
	Calculated data	Experimental data
1	254.8	249
2	258.4	253
3	264.6	259
4	269.1	264
5	278.2	271
6	285.5	280
7	291.9	287
8	298.1	294
9	302.5	299
10	308.7	304.5

Table 4

Influence of the cooling holes diameter d on the value of maximum dynamic stresses on the blade output edge

Holes diameter d, mm	Maximum dynamic stresses value σ, MPa	
	Calculated data	Experimental data
1.5	257.6	253
2.0	265.1	260
2.5	276.4	271
3.0	289.5	282
5.0	315.9	306

When analyzing the data, represented in Table 3, we can find the following dependence – with the increase of the cooling holes quantity, the value of the dynamic stresses on the blade output edge increases too. The explanation of this

dependence can be obtained due to the fact of the whole blade feather stiffness decrease with the increase of the cooling holes amount. The cause of the maximum dynamic stresses increase with the increase of the cooling holes diameter (Table 4) is the same.

6. Discussion of results of the study of dynamic stresses in the cooling blade feather

Analysis of the data, given in Table 1–4 gives us an opportunity to state that the main zones of maximum dynamic stresses are localized in the blade's feather cavity. The main reason for this phenomenon is the blade feather constructional inhomogeneity, caused by a net of cooling channels on its internal surface. These channels are space curvilinear surfaces, which correct modeling is rather difficult. That's why the cooling channels walls can be correctly described by eight-node curvilinear finite elements of hexahedron type. The bottom of the channels and the transition zones between the channels and blade feather surface are described by specially developed curvilinear finite elements. So, the problem of boundary gap between the finite elements, modeling the internal and external surface of blade feather is successfully solved. Special attention should be paid to the usage of the same finite elements for the purpose of the power and heat calculations. This gives an opportunity to improve the solution convergence and as a result to increase the reliability of the obtained results. But it also should be said; that the correct modeling of the blade feather input and output edges with a large radius on the base of the developed finite elements is rather difficult.

Comparing the calculated results with the experimental data (Table 1–4) gives us an opportunity to postulate a high reliability of the developed mathematical model and numerical algorithm, used for calculation. The experimental methodology is given in the paper [17].

So, the obtained data can be used in the marine engine building area by specialized enterprises and companies, such as GP NVKG «Zarya» – «Mashproekt» (Nikolaev, Ukraine).

The developed mathematical model and the obtained results show the influence of the blade feather constructional inhomogeneity on the maximum dynamic stresses value and their localization zones sizes. These researches are the extension of studying the vibration processes and stress-strain state in the rotors of marine gas turbine engines of high power. Subsequently, the developed mathematical model and obtained results can be used as a base for studying the whole turbine rotor stress-strain state, caused by complex vibration and heat loads.

7. Conclusions

1. It has been possible to find out the influence of gas turbine blade constructional inhomogeneity on the field of dynamic stresses on its surface. Localization zones of these stresses and their maximum values have also been established. The results of the research show that the main stress concentrators are located in transfer zones from the walls of cooling channels to the internal surface of blade feather. In these zones, the ratio of maximum dynamic stresses varies from 261 MPa to 284 MPa. But the value of such stresses does not exceed the blades material limit of endurance.

So, this gives us an opportunity to continue the research in the field of gas turbine blades fatigue processes, taking into consideration such parameter as the ultimate strength limit of the blade material.

2. On the base of special three-dimensional curvilinear finite elements, the new more correct mathematical model has been developed. The usage of such mathematical model gives an opportunity to find the dynamic stresses localization zones on the turbine blade feather, influenced both by vibration and thermal loads. It has also been found that the usage of this mathematical model gives an opportunity to reduce the number of iterations, needed for the convergence of solution by 10 % to 16 %, compared with the solution, based on the hexahedron finite elements usage.

3. Analysis of the obtained results and comparison with the experimental data confirm the adequacy of the developed mathematical model. The divergence of the obtained numerical and experimental data is within 10–12 %.

References

1. Samaras C. Emissions and lifetime estimation modeling of industrial gas turbines. M. Sc. Progress Review, Cranfield University, UK, 2009. P. 30–35.

2. Transient state stress analysis on an axial flow gas turbine blades and disk using finite element procedure / Sukhvinder K. B., Shyamala Kumari M. L., Neelapu M. L., Kedarinath C. // Proceedings of the 4th WSEAS Int. Conf. on Heat Transfer, Thermal Engineering and Enviroment. Elounda, Greece, 2006. P. 323–330.

3. Structural and Thermal Analysis of Gas Turbine Blade by using FEM / Krishnakanth P. V., Narasa Raju G. et. al. // International Journal of Scientific Research Engineering and Technology. 2013 Vol. 2, Issue 2. P. 060–065.

4. Mrinaline M. Steady state structural analysis of single crystal turbine blade // International Journal of Engineering Research and Technology. 2016. Vol. V5, Issue 10. P. 382–384. doi: 10.17577/ijertv5is100314

5. Ugargol R., Narayanaswamy K. S., Sesha Kumar C. V. Life estimation of turbine blisk for a gas turbine engine // International Journal of Mechanical Engineering and Technology. 2017. Vol. 8, Issue 8. P. 393–399.

6. Unsteady forces acting on the rotor blades in the turbine stage in 3D viscous flow in nominal and off-design regimes / Rzadkowski R., Gnesin V., Kolodyazhnaya L., Kubitz L. // Journal of Vibration Engineering, and Technologies. 2014. Vol. 2, Issue 2. P. 89–95.

7. Baqersad J., Niezrecki C., Avitabile P. Predicting full-field dynamic strain on a three-bladed wind turbine using three dimensional point tracking and expansion techniques // Sensors and Smart Structures Technologies for Civil, Mechanical, and Aerospace Systems 2014. 2014. doi: 10.1117/12.2046106

8. Theoretical and experimental stress-strain analysis of machining gas turbine engine parts made of the high energy structural efficiency alloy / Postnov V. V., Starovoitov S. V., Fomin S. Y., Basharov R. R. // Journal of Engineering Science and Technology Review. 2014. Vol. 7, Issue 5. P. 47–50.

9. Bitkina O., Kang K.-W., Lee J.-H. Experimental and theoretical analysis of the stress–strain state of anisotropic multilayer composite panels for wind turbine blade // Renewable Energy. 2015. Vol. 79. P. 219–226. doi: 10.1016/j.renene.2014.11.004

10. Kostyuk A. G. Dinamika i prochnost' turbomashin. Moscow: Mashinostroenie, 1982. 264 p.

11. Sosunov V. A., Chepkin V. M. Teoriya, raschet i proektirovanie aviacionnyh dvigateley i energeticheskih ustanovok. Moscow: Mosk. energ. in-t., 2003. 677 p.

12. Vorob'ev Yu. S. Kolebaniya lopatochnogo apparata turbomashin. Kyiv: Naukova dumka, 1988. 224 p.

13. Pyhalov A. A., Milov A. E. Staticheskiy i dinamicheskiy analiz sbornyh rotorov turbomashin. Irkutsk: Izd-vo Irkut. tekhn. un-ta, 2007. 194 p.

14. Morgun S. The blades constructions finite elements models development // Bulletin of the National Technical University «KhPI». Series: New Solutions in Modern Technologies. 2016. Issue 42 (1214). P. 86–91. doi: 10.20998/2413-4295.2016.42.14

15. Abramovich G. N. Prikladnaya gazovaya dinamika. Moscow: Nauka, 1991. 600 p.

16. Samarskiy A. A., Vabicevich P. N. Vychislitel'naya teploperedacha. Moscow: Editorial, 2009. 784 p.

17. Kairov A. S., Morgun S. A. Eksperimental'noe issledovanie peremennyh vibronapryazheniy v rabochih lopatkah turbomashin // Prohresyvni tekhnolohiyi i systemy mashynobuduvannia. 2013. Issue 1 (45)-2 (46). P. 131–138.